

Pair-breaking effects on the specific heat of a superconductor

P. J. Williams*

Physics Department, Mount Allison University, Sackville, New Brunswick, Canada E0A 3C0

(Received 11 January 1993)

We have studied the effect of static and dynamic pair breaking on the normalized-specific-heat jump of a superconductor. We find that in contrast to the static impurity case, dynamic pair breaking enhances the specific-heat jump. We have employed functional-derivative techniques in order to gain some understanding of this result.

I. INTRODUCTION

There is a substantial amount of experimental evidence that indicates that magnetism is important in the high- T_c oxide superconductors.¹⁻⁹ There have also been several theoretical proposals in which antiferromagnetic order or spin fluctuations have been incorporated.^{10,11} Varma *et al.*¹²⁻¹⁸ have proposed the marginal Fermi-liquid (MFL) model in which the electrons are supposed to interact via both charge and spin fluctuations. The charge fluctuations are attractive and the spin fluctuations are repulsive. Using this model, various normal and superconducting properties have been calculated.¹²⁻²⁵ The normal-state results are in very good agreement with the experimental data. This is perhaps not too surprising, as the model was constructed explicitly to describe the normal-state properties. The results for the superconducting state are also quite interesting. There is some disagreement over the expected size of the specific-heat jump that such a model would produce. Kuroda and Varma predict that the normalized-specific-heat jump, $\Delta C/C_N \approx 0.7$, smaller than the BCS value of 1.43. In addition, they also predict that the slope of the specific heat at T_c will be unusually large, although they do not make a quantitative prediction for this value. Williams and Carbotte¹⁹ have calculated the specific-heat jump and slope in a model in which there are two competing dynamical interactions, one which causes the superconductivity, and one which suppresses the superconductivity. Such a model is a generalization of the model of Ref. 14. In contrast to the results of Ref. 14, Williams and Carbotte find that while the slope is larger than the BCS value, the specific-heat jump is also enhanced over the BCS value.

In this paper, we extend the results of Williams and Carbotte to the extreme low-frequency limit for the spin fluctuations. We find that in the limit of the characteristic spin-fluctuation frequency tending to zero, the specific-heat jump is still enhanced over the BCS value. We employ functional-derivative techniques to gain some understanding of why the jump is enhanced for the dynamic pair breaking and suppressed for static pair breaking.

In Sec. II, we present the formalism used for the rest of the paper. Section III contains the numerical results for

the specific-heat jump and the slope of the specific heat at T_c . In Sec. IV, we present the functional-derivative calculations, and our conclusions are in Sec. V.

II. FORMALISM

The isotropic Eliashberg equations, written on the imaginary axis, including spin fluctuations are²⁶⁻²⁹

$$\Delta(i\omega_n)Z_s(i\omega_n) = \pi T \sum_{m=-\infty}^{\infty} \lambda^-(m-n) \frac{\Delta(i\omega_m)}{\sqrt{\Delta^2(i\omega_m) + \omega_m^2}} \quad (2.1)$$

and

$$\omega_n Z_s(i\omega_n) = \omega_n + \pi T \sum_{m=-\infty}^{\infty} \lambda^+(m-n) \frac{\omega_m}{\sqrt{\Delta^2(i\omega_m) + \omega_m^2}}, \quad (2.2)$$

where

$$\lambda^\pm(m-n) = 2 \int_0^\infty \frac{\omega [E(\omega) \pm P(\omega)]}{\omega^2 + (\omega_m - \omega_n)^2} d\omega. \quad (2.3)$$

$E(\omega)$ and $P(\omega)$ are the electron-boson (phonon, charge fluctuation, etc.) and electron-spin fluctuation spectral densities, respectively, and $i\omega_n = i\pi T(2n-1)$, $n \in I$ are the Matsubara frequencies. In our numerical work we have set the Coulomb pseudopotential μ^* to zero for simplicity, although we retain it in Sec. IV for the analytic work. Throughout we will denote the critical temperature of a pure system (no pair breaking, either static or dynamic) as T_c^0 and T_c will be used to denote the critical temperature of a system with pair breaking.

For both the boson and spin fluctuations we have employed Einstein spectral densities of the form

$$\begin{aligned} E(\omega) &= \frac{\omega_E \lambda^E}{2} \delta(\omega - \omega_E), \\ P(\omega) &= \frac{\omega_P \lambda^P}{2} \delta(\omega - \omega_P) \end{aligned} \quad (2.4)$$

with λ^E and λ^P the mass enhancement parameters for $E(\omega)$ and $P(\omega)$, respectively.

In order to calculate thermodynamic quantities we utilize the Bardeen-Stephen expression for the free-energy difference between the normal and superconducting states³⁰

$$F_n - F_s = N(0)\pi T \sum_{m=-\infty}^{\infty} \left[\sqrt{\tilde{\Delta}^2(i\omega_m) + \tilde{\omega}^2(i\omega_m)} - |\tilde{\omega}(i\omega_m)| \right] \times \left[1 - \frac{|\tilde{\omega}_m^0|}{\sqrt{\tilde{\Delta}^2(i\omega_m) + \tilde{\omega}^2(i\omega_m)}} \right],$$

$$\tilde{\omega}^0(i\omega_n) \equiv \omega_n + \pi T \sum_{m=-\infty}^{\infty} \lambda^+(m-n) \text{sgn} \omega_m. \quad (2.5)$$

The specific-heat jump is readily obtained from the free-energy difference through the standard thermodynamic relations and is given by

$$\frac{\Delta C}{\gamma T_c} = \frac{T}{\gamma T_c} \frac{d^2 \Delta F(T)}{dT^2}. \quad (2.6)$$

III. SPECIFIC-HEAT JUMP

We have solved Eqs. (2.1) and (2.2) numerically and used the results to calculate the specific heat given by Eq. (2.6). We chose a critical temperature of 200 K for the system with no spin fluctuations. We then added sufficient spin fluctuations to suppress the critical temperature to 100 K. We fixed $T_c^0/\omega_E = 0.1$ and let $0 < T_c^0/\omega_P < \infty$. We use the parameters T_c^0/ω_E and T_c^0/ω_P to discuss the results. It has been shown for materials that are well described by the Eliashberg formalism that the parameter T_c/ω_{in} can be used to characterize the superconducting properties of a material.³¹ ω_{in} is the Allen-Dynes parameter,³² and for Einstein spectra, $\omega_{\text{in}} \equiv \omega_E$.

In Fig. 1, we show numerical results for the normalized specific-heat jump, $\Delta C/\gamma T_c$, plotted versus T_c^0/ω_P . The curve starts off at 1.70, slightly above the BCS value of 1.43. This is due to the fact that $T_c^0/\omega_E = 0.1$, and for such a coupling strength, one expects to see an enhancement over the BCS value.³³ As T_c^0/ω_P increases, the specific-heat jump continues to increase, and appears to saturate at a value of ≈ 4.84 as T_c^0/ω_P approaches infinity. In order to investigate the trend as T_c is suppressed, we fixed ω_E , λ_E , and ω_P and then increased λ_P in order to suppress T_c . The results of these calculations are shown in Fig. 2 where the solid curve shows $\Delta c/\Delta c(T_c^0)$ versus T_c . $\Delta c \equiv \frac{\Delta C}{\gamma T_c}$ and $\Delta c(T_c^0) = 2.06$.

As the amount of pair breaking is increased, the curve increases, reaching a value of approximately 2.9 for $T_c/T_c^0 = 0.38$. The curve appears to be increasing more rapidly as T_c/T_c^0 decreases. We had to stop at this point due to numerical difficulties.

The dotted curve in Fig. 2 shows the Abrikosov-

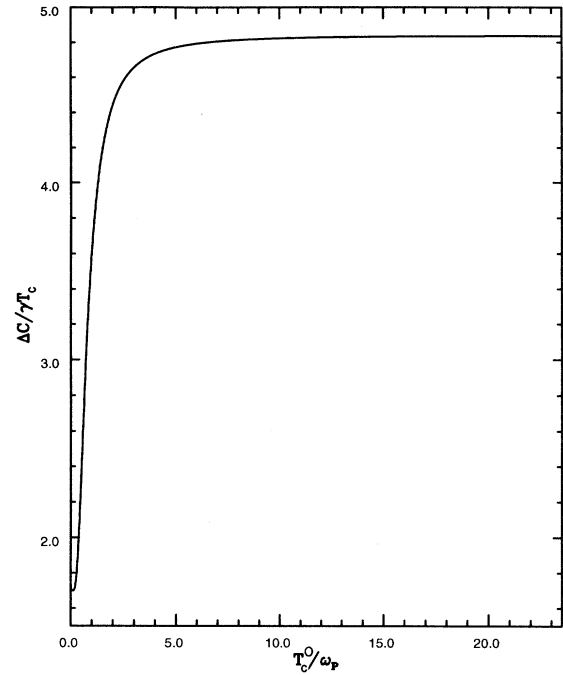


FIG. 1. Specific-heat jump vs T_c^0/ω_P . For this case, $T_c/T_c^0 = 0.5$, $T_c^0 = 200$ K, and $T_c^0/\omega_E = 0.1$. The curve appears to saturate at approximately 4.8 as $T_c^0/\omega_P \rightarrow \infty$. Hence, the extreme low-frequency limit for the pair breaking does not go over to the static limit.

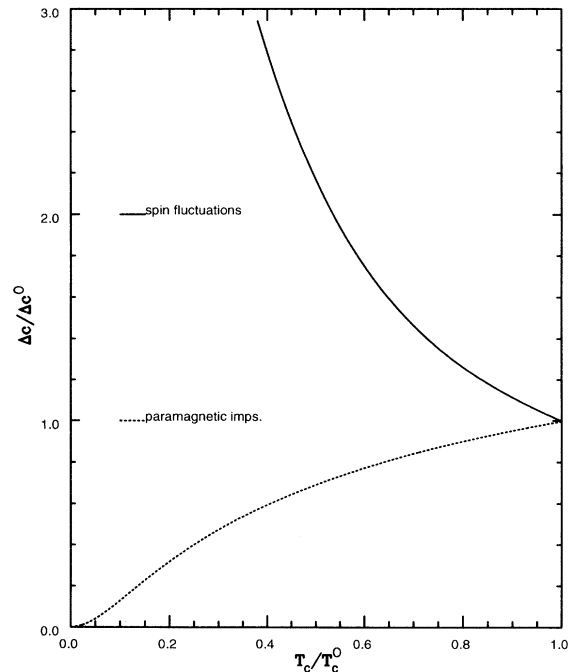


FIG. 2. $\Delta c/\Delta c^0$ vs $t = T_c/T_c^0$. $\Delta c \equiv \Delta C/\gamma T_c$ and Δc^0 is the jump at $t = 1$. The solid curve is for the case where the pair breaking is frequency dependent, while the dotted curve shows the Abrikosov-Gorkov results for paramagnetic impurities. For the dynamic case, the jump is everywhere enhanced over the pure value, while for the static case the jump is everywhere suppressed relative to the pure value.

Gorkov³⁴ results for $\Delta c/\Delta c(T_c^0)$ versus T_c/T_c^0 of a superconductor whose critical temperature is suppressed by static paramagnetic impurities. These results are valid in the BCS limit of $T_c^0/\omega_E=0$. Note that the trend is for $\Delta C/\gamma T_c$ to decrease as T_c decreases, exactly opposite to what occurs for the dynamic pair breaking.

IV. FUNCTIONAL DERIVATIVES

In order to gain more insight into the results of the previous section, we now consider the functional derivative of the specific-heat jump with respect to the spectral density

$$\frac{1}{\gamma} \frac{\delta(\Delta C/T_c)}{\delta A(\omega)} \equiv \frac{1}{\gamma} \lim_{\epsilon \rightarrow 0} \frac{(\Delta C/T_c)[A(\Omega) + \epsilon \delta(\Omega - \omega)] - (\Delta C/T_c)[A(\Omega)]}{\epsilon}.$$

$A(\omega)$ could be either $E(\omega)$ or $P(\omega)$. This quantity tells us about the sensitivity of the specific-heat jump to details of the spectral density function. Functional-derivative techniques were first employed in Eliashberg theory by Bergmann and Rainer,³⁵ who studied the derivative of the critical temperature with respect to the spectral density function. Since that work, the functional derivatives of many other superconducting properties have been studied.³⁶

In this work, rather than use full numerical solutions to calculate the functional derivatives, we will employ a square-well approximation^{37,38} ($\lambda^{\theta\theta}$ model)

$$\lambda(m-n) = \lambda(0)\Theta(\omega_D - |\omega_m|)\Theta(\omega_D - |\omega_n|), \quad (4.1)$$

where ω_D is the maximum frequency associated with the electron-boson interaction. In the case of the electron-phonon interaction, ω_D would be the Debye frequency. This model has the advantage that it yields analytical results which are largely independent of material parameters.

We will first calculate the derivative of $\Delta C/\gamma T_c$ in a model in which there is a single attractive dynamical interaction and a static repulsive interaction, due to paramagnetic impurities. For this case, $P(\omega)=0$ and hence $\lambda^+(m-n) = \lambda^-(m-n) = \lambda(m-n)$. The Eliashberg equations which we start with are

$$\bar{\Delta}(i\omega_n) = \pi T \sum_{m=-\infty}^{\infty} [\lambda(m-n) - \mu^*] \frac{\bar{\Delta}(i\omega_m)}{\sqrt{\bar{\Delta}^2(i\omega_m) + \bar{\omega}^2(i\omega_m)}} - \pi t^- \frac{\bar{\Delta}(i\omega_n)}{\sqrt{\bar{\Delta}^2(i\omega_n) + \bar{\omega}^2(i\omega_n)}}, \quad (4.1a)$$

$$\bar{\omega}(i\omega_n) = \omega_n + \pi T \sum_{m=-\infty}^{\infty} \lambda(m-n) \frac{\bar{\omega}(i\omega_m)}{\sqrt{\bar{\Delta}^2(i\omega_m) + \bar{\omega}^2(i\omega_m)}} + \pi t^- \frac{\bar{\omega}(i\omega_n)}{\sqrt{\bar{\Delta}^2(i\omega_n) + \bar{\omega}^2(i\omega_n)}}, \quad (4.1b)$$

$t^- = 1/2\pi\tau$, where τ is the magnetic scattering lifetime.

The calculation of the functional derivative of the specific-heat jump is done for temperatures near the critical temperature. Near T_c , the order parameter approaches zero and one may expand in powers of $\bar{\Delta}_n/\bar{\omega}_n$. To calculate the derivative at T_c it is sufficient to include terms up to second order in the Eliashberg equations. When expanding the free-energy equation, one must retain terms up to fourth order.

For this calculation it is useful to define

$$\bar{\Delta}(i\omega_n) = \bar{\Delta}(i\omega_n) \left[1 - \frac{\pi t^-}{\sqrt{\bar{\Delta}^2(i\omega_n) + \bar{\omega}^2(i\omega_n)}} \right]. \quad (4.2)$$

Expanding Eq. (4.2) to third order in $\bar{\Delta}_n/\bar{\omega}_n$ one obtains

$$\bar{\Delta}_n \simeq \frac{|\bar{\omega}(i\omega_n)|\bar{\Delta}(i\omega_n)}{|\bar{\omega}(i\omega_n)| + \pi t^-} \times \left\{ 1 + \frac{1}{2} \pi t^- \frac{|\bar{\omega}(i\omega_n)|}{|\bar{\omega}(i\omega_n)| + \pi t^-} \left[\frac{\bar{\Delta}(i\omega_n)}{\bar{\omega}_n} \right]^2 \right\}, \quad (4.3)$$

which is solved iteratively to obtain

$$\bar{\Delta}(i\omega_n) \simeq \frac{|\bar{\omega}(i\omega_n)|\bar{\Delta}(i\omega_n)}{|\bar{\omega}(i\omega_n)| + \pi t^-} + \frac{1}{2} \pi t^- \frac{|\bar{\omega}(i\omega_n)|\bar{\Delta}(i\omega_n)^3}{[|\bar{\omega}(i\omega_n)| + \pi t^-]^4}. \quad (4.4)$$

Rather than give complete details of the calculation, which are given elsewhere in the literature,³⁸ we will just give the main points. Within the $\lambda^{\theta\theta}$ model one finds that the gap function is independent of frequency, $\bar{\Delta}(i\omega_n) = \bar{\Delta}$. Solving (4.1a) and (4.1b) to lowest order, using Eq. (4.4), one obtains

$$1 = (A + \epsilon B) + (C + \epsilon D)\bar{\Delta}^2, \quad (4.5)$$

where A , B , C , and D are given in the Appendix.

It is useful at this point to carefully define the notation to be used for the various critical temperatures in the problem. The critical temperature for an impure material with a perturbed spectrum will be denoted by T_c^ϵ . The critical temperature for an impure material with an unperturbed spectrum will be denoted by T_c . Finally, the critical temperature for a pure material with an unperturbed spectrum is denoted by T_c^0 .

We now seek an expression for the free energy. The expansion of (2.5) to lowest order yields (after some straightforward but lengthy algebra)

$$\frac{F_s - F_n}{N(0)} = \frac{1}{2(\lambda - \mu^*)} \{C(T) + \epsilon D(T)\} \bar{\Delta}^4 \quad (4.6)$$

with C and D as in Eq. (4.5).

Equation (4.5) can be solved for $\bar{\Delta}^4$ and inserting this result into Eq. (4.6) and expanding about T_c , one obtains, to first order in ϵ ,

$$\begin{aligned} \frac{F_s - F_n}{N(0)} &= \frac{(T - T_c)^2}{2(\lambda - \mu^*)} \frac{A'^2}{C} \\ &\times \left[1 + \epsilon \frac{B'}{A'} - \epsilon \frac{1}{2} \frac{D}{C} - \epsilon \frac{A''B}{A'^2} \right. \\ &\quad \left. + \epsilon \frac{1}{2} \frac{BC'}{A'C} \right] \Bigg|_{T=T_c}. \end{aligned} \quad (4.7)$$

It then follows from equation (3.1) that the specific heat jump at T_c is given by

$$\begin{aligned} \frac{C_s - C_n}{C_n} &= -\frac{N(0)}{\gamma} \frac{1}{\lambda - \mu^*} \frac{A'^2}{C} \\ &\times \left[1 + \epsilon \frac{B'}{A'} - \epsilon \frac{1}{2} \frac{D}{C} - \epsilon \frac{A''B}{A'^2} \right. \\ &\quad \left. + \epsilon \frac{1}{2} \frac{BC'}{A'C} \right] \Bigg|_{T=T_c}. \end{aligned} \quad (4.8)$$

Defining $\Delta c \equiv (C_s - C_n)/C_n$, (4.8) may be written as

$$\Delta c^\epsilon = \Delta c_0 + \epsilon \Delta c_1$$

with the definitions of Δc_0 and Δc_1 obvious from (4.8). The functional derivative of the specific-heat jump at T_c is then given by

$$\begin{aligned} \frac{\delta \Delta c}{\delta E(\omega)} &= \Delta c_1, \\ \Delta c_1 &\equiv -\frac{N(0)}{\gamma} \frac{1}{\lambda - \mu^*} \frac{A'^2}{C} \\ &\times \left[\frac{B'}{A'} - \frac{1}{2} \frac{D}{C} - \frac{A''B}{A'^2} + \frac{1}{2} \frac{BC'}{A'C} \right] \Bigg|_{T=T_c}. \end{aligned} \quad (4.9)$$

If we write $\gamma = \frac{2}{3} \pi^2 N(0) (1 + \lambda)$, (4.9) becomes

$$\begin{aligned} \Delta c_1 &= -\frac{3}{2} \frac{1}{\pi^2 (1 + \lambda) (\lambda - \mu^*)} \frac{A'^2}{C} \\ &\times \left[\frac{B'}{A'} - \frac{1}{2} \frac{D}{C} - \frac{A''B}{A'^2} + \frac{1}{2} \frac{BC'}{A'C} \right] \Bigg|_{T=T_c}. \end{aligned} \quad (4.10)$$

Equation (4.10) appears to have an explicit $1/(\lambda - \mu^*)$ dependence, however, there is a factor of $\lambda - \mu^*$ in the sums, which cancels the prefactor. The cutoff has been relaxed as all the sums converge. This function is plotted in Fig. 3 versus ω/T_c^0 for various impurity concentrations, with $T_c/T_c^0 = 1.0, 0.9, 0.75$, and 0.5 for the solid, dotted, short-dashed, and long-dashed curves, respectively. The function is everywhere positive definite, and goes to zero in both the large and small limits of ω/T_c^0 limits.

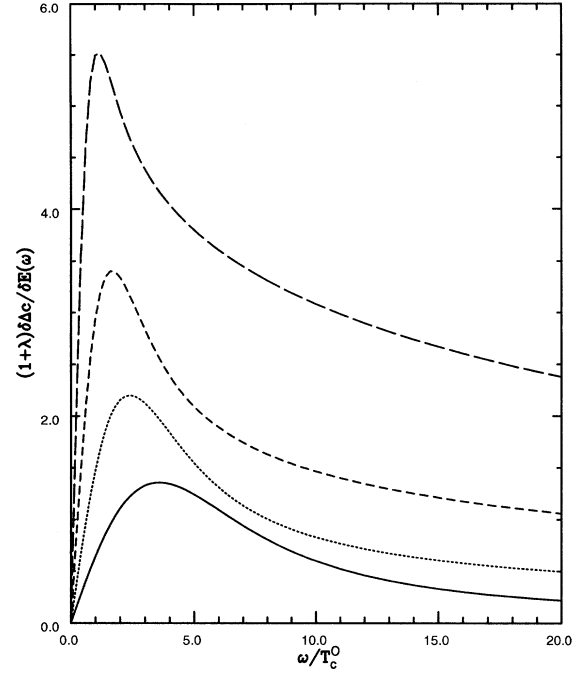


FIG. 3. Functional derivative of the specific-heat jump vs frequency, normalized to the critical temperature. The curves are all everywhere positive. The various curves are for different impurity concentrations, with $T_c/T_c^0 = 1.0, 0.9, 0.75$, and 0.5 for the solid, dotted, short-dashed, and long-dashed curves, respectively. The derivatives increase in size as the impurity concentration increases. This indicates that the suppression of the specific-heat jump increases more rapidly as the impurity concentration increases. This makes the added spectral weight more effective at larger concentrations.

The peak occurs for $\omega/T_c^0 \approx 4$ in the pure case. This peak softens as the impurity concentration is increased. The derivative also increases in size as the impurity concentration increases. This is understood by considering the dotted curve in Fig. 2, a plot of $\Delta c/\Delta c^0$ versus T_c/T_c^0 . Δc^0 is the specific-heat jump of the pure material. The specific-heat jump is being suppressed by the impurities and adding to the pairing spectral weight is somewhat analogous to reducing t^- .

We now contrast these results with those obtained in a model in which the pair breaking is dynamic rather than static. Marsiglio and Carbotte³⁸ have calculated the functional derivative of the specific-heat jump in such a case. They considered the derivative with respect to both the pairing and the depairing mechanism within the λ^{00} model. In their calculations, they treated the two mechanisms as distinct. Again, the details of the calculations are omitted, and we simply show their results in Fig. 4.

The solid curve is the functional derivative of the specific-heat jump with respect to the pairing spectra density [i.e., $E(\omega)$]. It is everywhere positive, with a broad peak at approximately $\omega/T_c = 3.5$. This result shows that adding spectral weight at any frequency will enhance the specific-heat jump. The dotted curve shows the functional derivative of the specific heat with respect

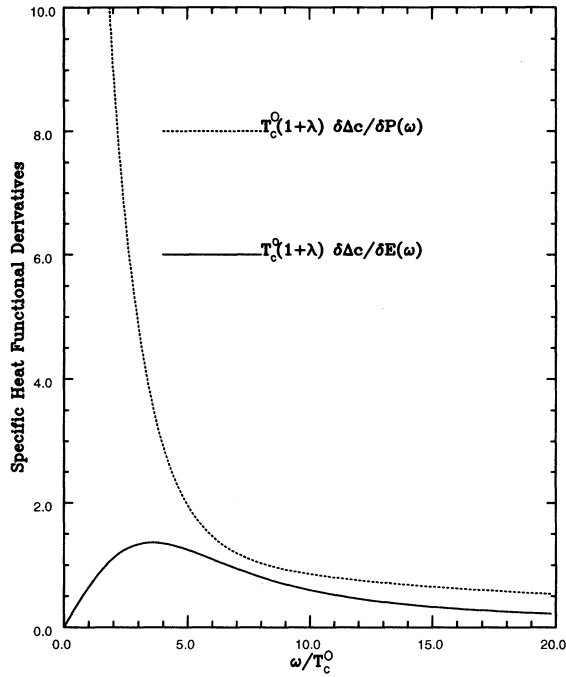


FIG. 4. Functional derivative of the specific-heat jump. The solid curve is the derivative with respect to the pairing spectral density. It is everywhere positive, indicating that adding spectral weight at any frequency will enhance the jump. The dotted curve is the derivative with respect to the pair-breaking spectral density. It is also everywhere positive, indicating that adding spectral weight at any frequency will enhance the jump. Adding spectral weight at low frequencies is particularly effective.

to the depairing mechanism. It is everywhere positive definite, and diverges to positive infinity at low frequencies. This indicates that adding paramagnon spectral weight will also enhance the specific-heat jump, but that adding weight at low frequencies is particularly effective in enhancing the jump.

Williams and Carbotte³⁹ have numerically calculated the functional derivative of the specific-heat jump in a model where the same fluctuations couple the electrons via both charge and spin, as in the MFL model. In this case, the spectra function, say $A(\omega)$, for both the pairing and the depairing is the same, with the exception that they have different weights. To be explicit, if we define the parameter $g = (\lambda_e - \lambda_p) / (\lambda_e + \lambda_p)$ then

$$P(\omega) = \frac{1-g}{1+g} E(\omega) \quad (4.11)$$

and

$$\frac{1}{\gamma} \frac{\delta(\Delta C/T_c)}{\delta A(\omega)} = \frac{1}{\gamma} \frac{\delta(\Delta C/T_c)}{\delta E(\omega)} + \frac{1-g}{\gamma(1+g)} \frac{\delta(\Delta C/T_c)}{\delta P(\omega)}. \quad (4.12)$$

We show the results of these calculations in Fig. 5. These curves are essentially a combination of the curves from Fig. 4, with different values of g corresponding to

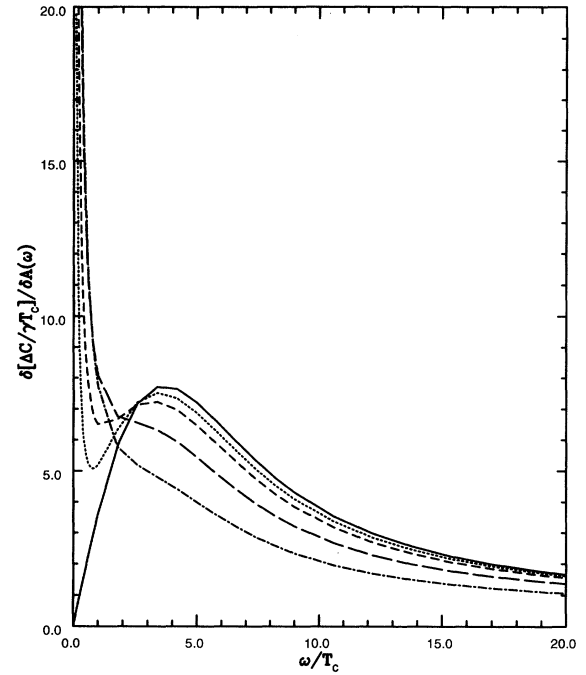


FIG. 5. Functional derivative of the specific-heat jump for a model in which the pairing and pair-breaking spectral densities are the same. The solid, dotted, short-dashed, long-dashed, and dash-dotted curves correspond to $g = 1.0, 0.95, 0.9, 0.8,$ and 0.7 , respectively. These derivatives are everywhere positive definite, indicating that in such a model, the specific-heat jump will be enhanced over the value for a model in which there is no pair breaking.

different relative weights of the two curves in Fig. 4.

Hence, in a system where there is both pairing and depairing, adding spectral weight to either spectral function will enhance the specific-heat jump. This is consistent with the results shown in Fig. 1. Note also in Fig. 5 that the derivative is suppressed at higher frequencies. This is due to the fact that the specific-heat jump is already enhanced and enhancing it further becomes difficult.

V. CONCLUSIONS

In Sec. III, we showed that for a model in which the pair breaking is dynamic, the normalized-specific-heat jump is enhanced over the value that one would obtain if there was no pair breaking. This is in contrast to the case where there is static pair breaking, as with paramagnetic impurities. In such a case, the normalized-specific-heat jump is depressed over the pure value.

These results can be understood in terms of the functional derivatives of the normalized-specific-heat jump with respect to the spectral density functions. For the dynamic case, the functional derivative of the normalized-specific-heat jump is positive definite at all frequencies for both the pairing and the depairing mecha-

nism. This means that both mechanisms tend to enhance the normalized-specific-heat jump. The positive divergence at low frequencies of the derivative with respect to the depairing mechanism shows that low frequencies are particularly effective in enhancing the jump.

The derivatives for the static case are again everywhere positive definite. They increase in size as the amount of pair breaking increases. This indicates that the normalized-specific-heat jump is being more rapidly suppressed with larger impurity concentration, and add-

ing the spectral weight becomes more and more effective in enhancing the jump over its suppressed value.

There are available experimental results⁴⁰ in which the specific-heat jump is studied as a function of T_c . In these experiments, T_c is being suppressed by adding Fe and Zn in place of Cu in YBCO materials. The specific-heat jump decreases as T_c decrease. We would interpret this as meaning that Fe and Zn are acting as paramagnetic impurities and are not leading to any dynamical pair-breaking effects.

APPENDIX

Below are given the functions A , B , C , and D which appear in the T_c equation as well as the expansion for the free energy given in Sec. IV:

$$A = \pi T \sum_{m=-N_c}^{N_c} (\lambda - \mu^*) \frac{1}{|\bar{\omega}(i\omega_m)|}, \quad (\text{A1})$$

$$B = (\pi T)^2 \sum_{m=-N_c}^{N_c} (\lambda - \mu^*) \frac{1}{|\bar{\omega}(i\omega_m)|} \sum_{m'=-\infty}^{\infty} \delta\lambda(m' - m) \frac{1}{|\bar{\omega}(i\omega_m)|} - (\pi T)^2 \sum_{m=-\infty}^{\infty} \frac{f_m}{|\bar{\omega}(i\omega_m)|^2}, \quad (\text{A2})$$

$$C = \pi^2 T^2 t^{-} \sum_{m=-N_c}^{N_c} (\lambda - \mu^*) \frac{1}{|\bar{\omega}(i\omega_m)|^4} - \frac{1}{2} \pi T \sum_{m=-N_c}^{N_c} (\lambda - \mu^*) \frac{1}{|\bar{\omega}(i\omega_m)|^3}, \quad (\text{A3})$$

$$\begin{aligned} D = & 4\pi^3 T^2 t^{-} \sum_{m=-N_c}^{N_c} (\lambda - \mu^*) \frac{1}{|\bar{\omega}(i\omega_m)|} \sum_{m'=-\infty}^{\infty} \delta\lambda(m' - m) \frac{1}{|\bar{\omega}(i\omega_m)|^4} \\ & - 2(\pi T)^2 \sum_{m=-N_c}^{N_c} (\lambda - \mu^*) \frac{1}{|\bar{\omega}(i\omega_m)|} \sum_{m'=-\infty}^{\infty} \delta\lambda(m' - m) \frac{1}{|\bar{\omega}(i\omega_m)|^3} \\ & + \frac{1}{2} (\pi T)^2 \sum_{m=-N_c}^{N_c} (\lambda - \mu^*) \frac{1}{|\bar{\omega}(i\omega_m)|^2} \sum_{m'=-\infty}^{\infty} \delta\lambda(m - m') \text{sgn}(\omega_m \omega_{m'}) \frac{1}{|\bar{\omega}(i\omega_m)|^2} \\ & - 4\pi^3 T^2 t^{-} \sum_{m=-N_c}^{N_c} (\lambda - \mu^*) \frac{f_m}{|\bar{\omega}(i\omega_m)|^5} + \frac{3}{2} (\pi T)^2 \sum_{m=-N_c}^{N_c} (\lambda - \mu^*) \frac{f_m}{|\bar{\omega}(i\omega_m)|^4}. \end{aligned} \quad (\text{A4})$$

*Current address: Physics Department, Acadia University, Wolfville, Nova Scotia, Canada B0P 1X0.

¹Y. Kitaoko, S. Hiramatsu, K. Ishida, T. Kohara, and K. Asayama, *J. Phys. Soc. Jpn.* **56**, 3024 (1987); Y. Kitaoko, K. Ishida, S. Hiramatsu, and K. Asayama, *ibid.* **57**, 734 (1988).

²I. Wanatabe, K. Kumagai, Y. Nakamura, T. Kimura, Y. Nakamichi, and H. Nakajima, *J. Phys. Soc. Jpn.* **56**, 3028 (1987).

³D. Vagnin, S. K. Sinha, D. E. Moncton, D. C. Johnston, J. M. Newsam, C. R. Safinya, and H. E. King, Jr., *Phys. Rev. Lett.* **58**, 2802 (1987).

⁴Y. J. Uemura, W. J. Kossler, X. H. Yu, J. R. Kempton, H. E. Schone, D. Opie, C. E. Stronach, D. C. Johnston, M. S. Alvarez, and D. P. Goshorn, *Phys. Rev. Lett.* **58**, 1045 (1987).

⁵J. I. Budnick, B. Chamberland, D. P. Yang, Ch. Neidermayer, A. Golnik, E. Recknagel, M. Rossmannith, and A. Weidinger, *Europhys. Lett.* **5**, 651 (1988); J. I. Budnick, A. Golnik, Ch. Neidermayer, E. Recknagel, M. Rossmannith, A. Weidinger, B. Chamberland, M. Filipkowski, and D. P. Yang, *Phys. Lett. A* **124**, 103 (1987).

⁶J. H. Brewer *et al.*, *Phys. Rev. Lett.* **60**, 1073 (1988).

⁷P. W. Anderson, *Science* **235**, 1196 (1987); P. W. Anderson, G. Baskaran, Z. Zhou, and T. Hsu, *Phys. Rev. Lett.* **58**, 2790 (1987).

⁸V. I. Emery, *Phys. Rev. Lett.* **58**, 2794 (1987).

⁹M. Cyrot, *Solid State Commun.* **62**, 821 (1987).

¹⁰J. R. Schrieffer, X.-G. Wen, and S.-C. Zhang, *Phys. Rev. Lett.* **60**, 944 (1988).

¹¹A. Aharony, R. J. Birgeneau, A. Coniglio, M. A. Kastner, and H. E. Stanley, *Phys. Rev. Lett.* **60**, 1330 (1988); R. J. Birgeneau, M. A. Kastner, and A. Aharony, *Z. Phys. B* **71**, 57 (1988).

¹²A. Weidinger, Ch. Niedermayer, A. Golnik, R. Simon, E. Recknagel, J. I. Budnick, B. Chamberland, and C. Baines, *Phys. Rev. Lett.* **62**, 102 (1989).

¹³C. M. Varma, *Int. J. Mod. Phys. B* **3**, 2083 (1989).

¹⁴C. M. Varma, P. B. Littlewood, S. Schmitt-Rink, E. Abrahams, and A. Ruckenstein, *Phys. Rev. Lett.* **63**, 1996 (1989).

¹⁵C. M. Varma, S. Schmitt-Rink, and E. Abrahams, *Solid State Commun.* **62**, 681 (1987).

- ¹⁶P. B. Littlewood, C. M. Varma, S. Schmitt-Rink, and E. Abrahams, *Phys. Rev. B* **39**, 12 371 (1989).
- ¹⁷Y. Kuroda and C. M. Varma, *Phys. Rev. B* **42**, 8619 (1990).
- ¹⁸P. J. Williams and J. P. Carbotte, *Phys. Rev. B* **43**, 7960 (1991).
- ¹⁹E. J. Nicol, J. P. Carbotte, and T. Timusk, *Phys. Rev. B* **43**, 473 (1991); *Solid State Commun.* **76**, 937 (1990).
- ²⁰E. J. Nicol and J. P. Carbotte, *Phys. Rev. B* **43**, 1158 (1991).
- ²¹E. J. Nicol and J. P. Carbotte, *Solid State Commun.* **78**, 55 (1991).
- ²²P. B. Littlewood and C. M. Varma, *Phys. Rev. B* **46**, 405 (1992).
- ²³P. B. Littlewood and C. M. Varma, *J. Appl. Phys.* **69**, 4979 (1991).
- ²⁴E. J. Nicol and J. P. Carbotte, *Phys. Rev. B* **44**, 12 511 (1991).
- ²⁵E. J. Nicol and J. P. Carbotte, *Phys. Rev. B* **44**, 7741 (1991).
- ²⁶J. M. Daams and J. P. Carbotte, *Solid State Commun.* **43**, 263 (1981).
- ²⁷J. M. Daams, B. Mitrović, and J. P. Carbotte, *Phys. Rev. Lett.* **46**, 65 (1981).
- ²⁸J. Baquero, J. M. Daams, and J. P. Carbotte, *J. Low Temp. Phys.* **42**, 585 (1981).
- ²⁹H. G. Zarate and J. P. Carbotte, *J. Low Temp. Phys.* **57**, 291 (1984).
- ³⁰J. Bardeen and M. Stephen, *Phys. Rev.* **136**, A1485 (1964).
- ³¹B. Mitrović, H. G. Zarate, and J. P. Carbotte, *Phys. Rev. B* **29**, 184 (1984).
- ³²P. B. Allen and R. C. Dynes, *Phys. Rev. B* **12**, 905 (1975).
- ³³J. Blezius and J. P. Carbotte, *Phys. Rev. B* **36**, 3622 (1987).
- ³⁴See, for example, K. Maki, in *Superconductivity*, edited by R. D. Parks (Dekker, New York, 1961), Vol. 1, Chap. 3.
- ³⁵G. Bergmann and D. Rainer, *Z. Phys.* **263**, 59 (1974).
- ³⁶J. P. Carbotte, *Rev. Mod. Phys.* **62**, 1027 (1990).
- ³⁷P. B. Allen and B. Mitrović, *Solid State Phys.* **37**, 1 (1982).
- ³⁸F. Marsiglio and J. P. Carbotte, *Phys. Rev. B* **31**, 4192 (1985).
- ³⁹P. J. Williams and J. P. Carbotte, *Phys. Rev. B* **39**, 2180 (1989).
- ⁴⁰C. Mengast *et al.*, *Physica C* **173**, 309 (1991).